PAM Review
Subject 68412 www.uts.edu.au

Reviewing the relationship between thermal reservoir parameters and geothermal energy output

Jamie Grippi [1]

University of Technology Sydney, Faculty of Science, PO Box 123, Ultimo NSW 2007, Australia
[1] 12462368@uts.edu.au
DOI: http://dx.doi.org/10.5130/pamr.v5i0.1494

Abstract: This meta-study draws upon contemporary literature to examine parameters of thermal reservoirs and their relationships to geothermal power station output metrics. The objectives of the meta-study are to identify trends and quantify the influence of each parameter on the system as a whole. This study provides a framework for industry and researchers exploring new potential geothermal fields. Six reservoir parameters – well depth, temperature, enthalpy, mass flow rate, thermal gradient and crust thickness – were plotted against the net electrical output per production well ($E_{net/well}$) and exergy efficiency (η_B) of 64 geothermal facilities. The meta-study identified that reservoir temperature has the greatest proportionality to power output, with yields above 10MWe exhibited only for high enthalpy reservoirs exceeding 500K. Well depth has the greatest inverse proportionality to exergy efficiency, with upper limit values declining below 80% for wells deeper than 3000m. Well depth has a similar trend line, though lesser correlation, as reservoir temperature to power output. Crust thickness has an inverse correlation to exergy efficiency, with upper limit values dropping from 100% to 65% as thickness increased from 30 to 45km. There was significant clustering of data points in most trendless plots, suggesting a considerable degree of homogeneity between currently tapped reservoirs and turbine efficiencies. The low number of well-defined data trends implies a high degree of complexity arising from the relationships between reservoir parameters that make quantification problematic. Despite this difficulty, examination of the aforementioned parameters suggests that although hotter reservoirs are usually found at greater depths, the hottest and shallowest reservoirs should be prioritized for use in order to return maximal power outputs and reduce exergy losses that occur along large lengths of piping.

Keywords: geothermal energy; thermal reservoir; renewable energy; meta-study

Citation: Grippi, J. 2018. Reviewing the relationship between thermal reservoir parameters and geothermal energy output, PAM Review: Energy Science & Technology, Vol. 5, pp. 2-21. http://dx.doi.org/10.5130/pamr.v5i0.1494
PAM Review **is a UTS ePRESS Student Journal showcasing outstanding student works.**

Nomenclature

Geothermal Energy	Energy available in the Earth's crust
Thermal Reservoir	Region of heated liquid or gas in the Earth's crust
Geothermal Fluid	Heated liquid or gas in thermal reservoir
Geothermal System	Geothermal Power Station of undefined category
SF/DF	Single or Double Flash Geothermal Power Station
BK	Binary Kalina Cycle Geothermal Power Station
BORC	Binary Organic Rankine Cycle Geothermal Power Station
Well Depth, D_{well}	Distance from ground surface to thermal reservoir (m)
Temperature, T_{res}	Maximum temperature of geothermal fluid (K)
Enthalpy, H_{res}	Maximum enthalpy of geothermal fluid (kJ/kg)
Mass Flow Rate, F_{res}	Rate of geothermal fluid flow from reservoir to well piping (kg/s)
Thermal Gradient, G	Temperature increase per meter from ground surface to reservoir (K/m)
Crust Thickness, C	Distance from ground surface to bottom of Earth's crust
E_{cap}, $E_{cap/well}$	Electrical power production capacity of a geothermal system (E_{cap}) or per well of a geothermal system ($E_{cap/well}$), (MWe, megawatts per hour)
E_{net}, $E_{net/well}$	Real electrical power production of a geothermal system (E_{net}) or per well of a geothermal system ($E_{net/well}$), (MWe, megawatts per hour)
η_B	Exergy efficiency, proportion of E_{net} to E_{cap} of a geothermal system (%)

1. Introduction

Geothermal energy refers to heat available in the Earth's crust. This heat is produced in approximately equal proportions from high core temperatures caused by the initial formation of the planet and the radioactive decay of matter [1]. This energy can be utilized by pumping geothermal fluids, heated gases or liquids found in deep thermal reservoirs, into geothermal systems that contain steam-powered turbines to produce electricity that is directly supplied to the grid. A generalized schematic of a geothermal system is available in Figure 1, displaying the extraction of geothermal fluid from a heated reservoir, conversion to electricity, supply to the generator and transformer and finally condensing or cooling of the fluid for reinjection to the reservoir.

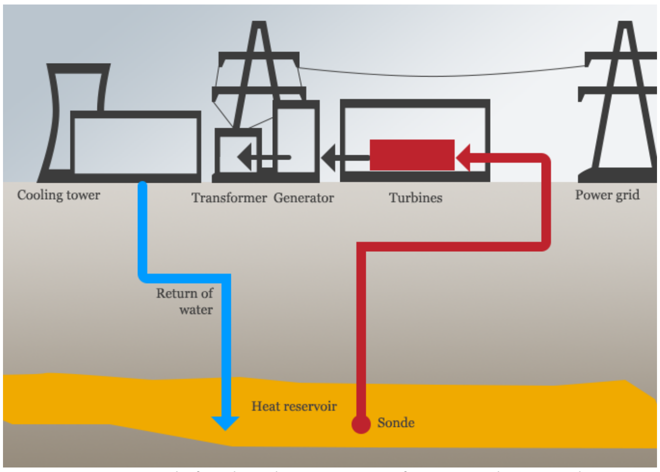

Figure 1. *Simplified schematic of a geothermal system* [2].

Geothermal systems are an advantageous branch of renewable energy production compared to fossil fuels due to minimal greenhouse emissions, producing less than 5% the CO_2 per kWh of common coal plants [3]. The few solid mineral byproducts of geothermal systems are readily extractable to be sold for use in commercial and industrial applications [4]. Liquid byproducts are often reinjected into the Earth in order to maintain the reservoir enthalpy (H_{res}), energy contained in a kilogram of geothermal fluid, and reservoir mass flow rate (F_{res}), kilograms of geothermal fluid movement per second past a defined point [5].

Thermal reservoirs fall into three enthalpy categories - low, medium and high - corresponding to geothermal fluid temperatures of 323-373K, 373-525K and above 525K [6]. Thermal gradient (G) is defined as a function of T_{res} to D_{well} in order to quantify temperature increase per meter of depth increase - however this is not likely to have a significant outcome on performance metrics as the theorized proportionality of these two parameters will likely return very small values. Crust thickness (C) is defined as the depth from ground surface level to the bottom of the Earth's crust layer, and higher C values are likely to result in higher G values as heat can more readily flow towards the surface.

Geothermal facilities exhibit a high degree of scalability due to their low physical footprint [7], making them ideal for use in urban areas where the pollutant byproducts of fossil fuels would be destructive. This scalability, and a >90% energy production uptime [8], or availability factor, heavily contributes to their potential for use as grid-stabilizers. As a widely connected grid is more prone to a cascading failure and power outage, geothermal facility dispersion across the world can provide an important energy supply backbone to reduce chances of these failures. The high initial outlay costs associated with establishing a geothermal plant warrant significant consideration in choosing new geothermal thermal fields for utilization [9].

Economics aside, a major drawback to the global expansion of geothermal energy production is the power stations substantial location dependency. This problem arises because performance is based on the thermodynamic parameters of reservoirs such as reservoir temperature (T_{res}) and well depth (D_{well}), in addition to H_{res} and F_{res}. This barrier affects the widespread formation of new geothermal power stations as the parameters of reservoirs in a geothermal field must be understood to a high degree of accuracy for the system to be thermodynamically feasible for use. The four aforementioned parameters contribute almost entirely to the performance outputs of a geothermal system, and thus geological surveyors must understand the importance of each.

Binary Cycle and Flash Steam plants are the most common under-construction and in-operation types of systems, respectively [10]. As shown in Figure 2a, Flash Steam plants rely on a moderately heated liquid passing through either one (Single Flash, SF) or multiple (Double Flash, DF) high-pressure separators that catalyze vaporization by rapidly dropping the pressure of the fluid in order to power a turbine and supply electricity to the grid. Exergy losses in Flash Steam plants often exceed 50%, with optimization occurring through a slight reduction in separator pressure [11].

Binary Cycle plants, as represented in Figure 2b, generally rely on lower enthalpy liquid passing through an intermediate tank in order to heat a secondary working fluid. This fluid has a lower specific heat capacity and boiling point that vaporizes the fluid, powering a turbine and supplying electricity to the grid. Binary Organic Rankine Cycle (BORC) plants are a type of Binary Cycle plant that utilizes a pure organic high molecular mass fluid as their working fluid. Binary Kalina (BK) plants differ from BORC plants, and contain a 2 fluid mixture for their working fluid, generally NH_3 and H_2O - though both operate on the same Binary Cycle principles. BORC systems present average exergy losses exceeding 50% from numerous sources, primarily condensers and vaporizers [12]. BK systems exhibit lower exergy losses of approximately one third of total exergy in, attributed in near-equal parts to the Kalina turbine, geothermal vapor turbine and across the heat exchangers [13].

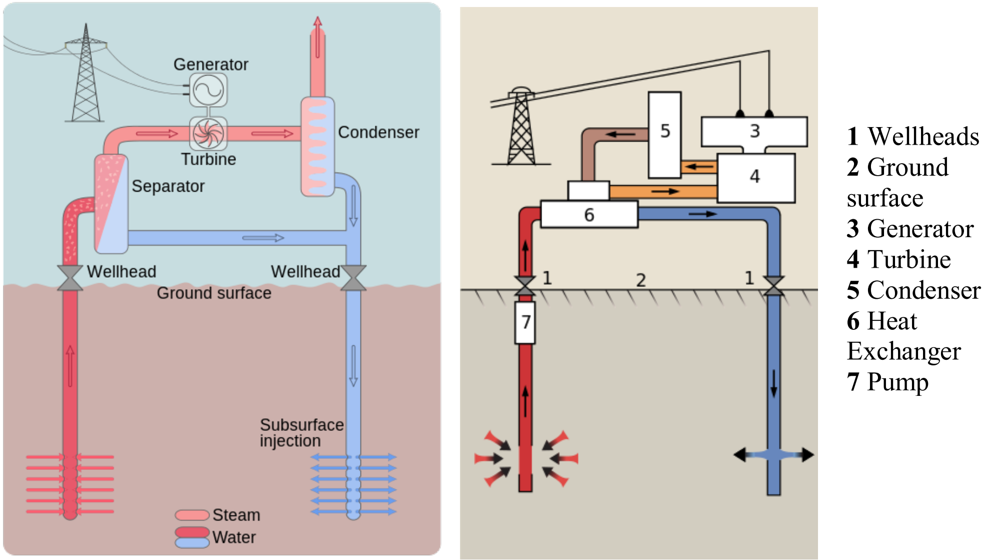

Figure 2. *Schematic of a* ***(a)*** *Flash Steam and* ***(b)*** *Binary Cycle GS* [14, 15].

Despite a current reliance of only 0.67% on geothermal renewables [16], researchers and industry-affiliated organizations have identified a worldwide total of $2x10^{24}W$ potential useable geothermal energy - enough to meet the world's current energy demands for multiple millennia [17]. With a massive potential for growth in this relatively unexploited renewable energy industry, it is imperative that geological surveyors can accurately and efficiently identify reservoirs and locations that would be economically and thermodynamically favorable for establishing new geothermal systems. Figure 3 illustrates how the highest risk for new geothermal project failure occurs in the first four stages before well-field development, dropping off significantly after this. Here we investigated six parameters of thermal reservoirs and their relation to power output metrics, net electrical output per well ($E_{net/well}$) and exergy efficiency (η_B), in order to identify trends and quantify the influence of each parameter on the system as a whole. With this, we are aiming to provide an approximate framework for industry and researchers exploring new locations.

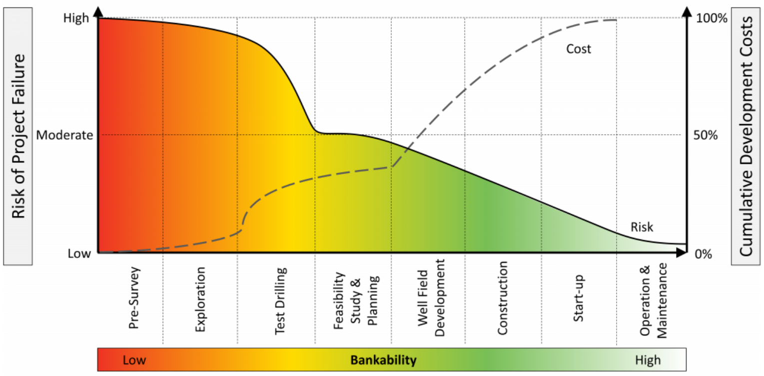

Figure 3. *Risk of project failure vs. cumulative development costs with bankability rating identified by colouring* [18].

2. Methodology

This meta-study draws on literature concerning reservoir thermodynamics and geothermal energy production. Sources were accessed via Google Scholar, Access Science, ProQuest Science & Technology, Science Direct, SCOPUS and the Web of Science Core Collection. Literature selection criteria and data acquisition involved cross-referencing between industry websites, government organizations, review papers and original research. The object was to obtain relevant insights into the industry trends and precise figures for specific geothermal systems. There was an emphasis on material produced since 2005, ensuring the relevance of collected data due to rapid advancements in turbine technology.

A gap in the literature was identified concerning the classification of the effects that thermal reservoir parameters have on the net output and exergy efficiency of geothermal power systems. The extensive body of knowledge currently available was utilized to investigate this gap and provide a framework for geological surveyors looking to accurately identify the thermal reservoirs that are most likely to be thermodynamically, and thus economically, viable. Six data metrics were extracted and tabulated (Appendix 1) from over 70 sources – reservoir temperature, depth, mass flow rate, enthalpy, crust thickness and installed electrical output capacity – for a total of 64 Binary Cycle and Flash systems, due to their standing as the most common types of GS under construction and in use, respectively.

The turbines utilized by different geothermal systems function in the same manner, despite differences between input methods, allowing for a generalized comparison of input to output metrics. From these metrics, the net electrical output per well ($E_{net/well}$) was calculated using Equation 1, where GWh is net energy produced yearly and W is number of wells, with transformation to Mwe by multiplication of 1000 MW per GW and division by 8760 hours per year. Exergy efficiency (η_B) was calculated using a simple derivation of the initial Equation 2, by dividing the net electrical output (E_{net}) of a power station by its theoretical electrical production capacity (E_{cap}). This efficiency equation is based on the principles of the Carnot Cycle (Appendix 2) that take into account the 2nd Law of Thermodynamics – that is, the quality of energy, energy degradation, entropy generation and work opportunity losses [19]. Equation 3 defines the relationship between the amount of heat transferred from a hot reservoir to a Carnot system, where Q_H is heat transferred to system, T_H is temperature of matter from the reservoir and S_A and S_B are the initial and final entropy states of the system.

$$\mathrm{E_{net}} = \left(\frac{\mathrm{GWh} \times 1000}{8760}\right) \div \mathrm{W} \qquad \text{Eq. 1}$$

$$\eta_B = \frac{W}{Q_H} = 1 - \frac{T_C}{T_H} \approx \frac{\mathrm{E_{net}}}{\mathrm{E_{cap}}} \qquad \text{Eq. 2}$$

$$Q_H = T_H(S_B - S_A) \qquad \text{Eq. 3}$$

Reservoir parameters were initially plotted against each other to identify if any coactive relationships exist between them and determine if normalization would be useful in data presentation, though no proportional trends were acknowledged. The only normalization of data was the presentation of net and installed capacity power output as a function of the number of wells ($E_{net/well}$ and $E_{cap/well}$), whereas η_B values were calculated from the total E_{net} and E_{cap} values of a power station. Out of 64 geothermal facilities analyzed, 28 had no enthalpy data available or calculable and 8 were missing mass flow rate data, excluding them from their respective plots. No distinction is made between traditional and enhanced geothermal systems, though enhanced systems can generally be taken as those with tapped wells above 2500m depth [20]. Crust thickness values were acquired via Figure 2, though an error margin of ±2.5km is noted due to the large tile sizes in the figure and 5km increments per tile classification. Linear trendlines were only fitted to plots where there is an easily identifiable trend to the naked eye, i.e. the trends identified as primary and secondary parameters. All reservoir parameters were plotted against each other and against $E_{net/well}$ and η_B to identify trends and quantify and rank each parameter's influence on output for the industry and researchers consideration in the exploration of new underground potential production wells.

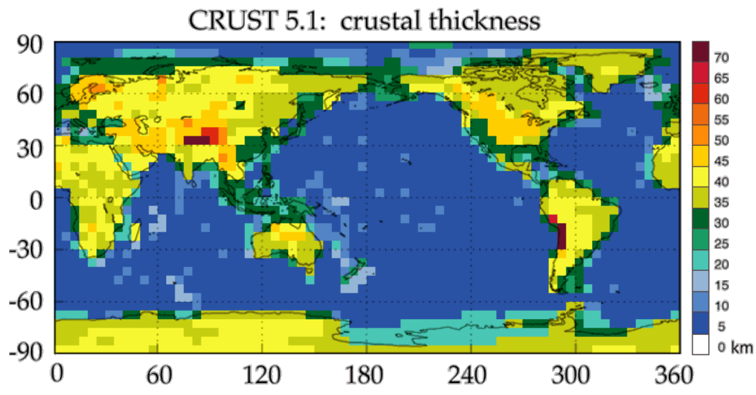

Figure 4. *Crustal thickness, tile size 5x5 degrees* [21].

3. Results and Discussion

A search of 50 papers on the topic of geothermal power output returned only 3 papers involving an explicit focus on thermal reservoir conditions as they influence output metrics, with many papers examining optimal working fluids for binary plants and turbine thermal efficiencies. No papers were found that focused on all four main thermal reservoir parameters - well depth, temperature, enthalpy and mass flow rate. This meta-study attempts to fill this gap in the literature by identifying trends in these four thermal reservoir parameters as well as crust thickness and thermal gradient as they relate to each other, and to the output metrics of geothermal systems. The influence of the aforementioned parameters on output metrics renders their classification as being primary, secondary or tertiary in nature in order of descending relationship strength.

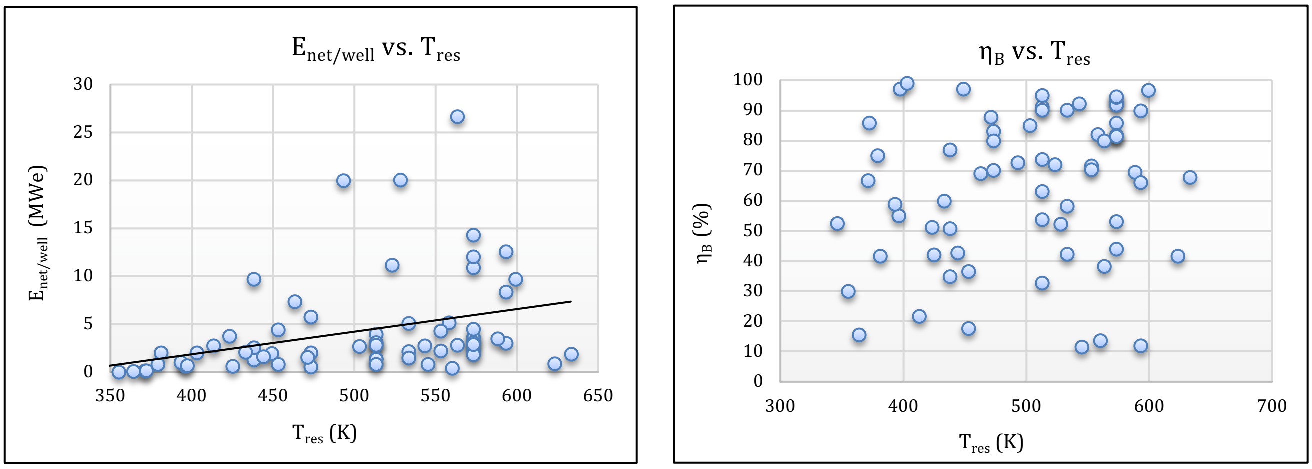

Figure 5. (a) *$E_{net/well}$ as a function of T_{res}* **(b)** *η_B as a function of T_{res}*.

Figure 5a, a plot of T_{res} to $E_{net/well}$, exhibits the strongest trend of a thermal reservoir parameter to power output, with no facilities exceeding 10MWe per well for reservoirs below 490K, i.e. low and medium enthalpy reservoirs. This trend was expected as steam turbines operate on the principles of the Carnot Cycle, as defined in Equation 3. The equation states that the total thermal energy transferred from a hot reservoir to a system is the product of the reservoir fluid temperature and the change in entropy of the system from its initial to final state. Due to this equation, and temperature having a higher magnitude than entropy due to the nature of their definitions and units, it is clear how T_{res} has the most distinct effect on the power output of a geothermal system compared to the other five investigated parameters. Figure 5b was expected to exhibit a similar trend to that of 5a, as an increase in input temperature or decrease in exhaust temperature of a system leads to efficiency increasing, as defined by the Carnot engine efficiency equation in Equation 2. T_{res} was found to have no correlation to η_B, with a random scattering of data points across the plot with no discernible proportionality of any kind.

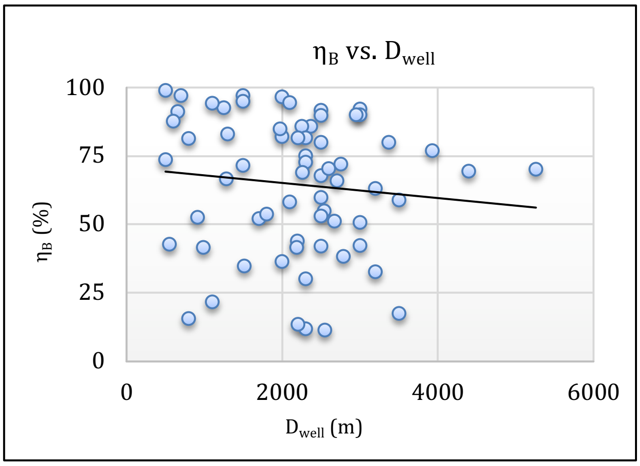

Figure 6. (a) *$E_{net/well}$ as a function of D_{well}* **(b)** *η_B as a function of D_{well}.*

The discrepancy between the trends in the Figure 5 plots appears to be explained by the exergy trend shown in Figure 6b. These losses theoretically occur through the walls of the large lengths of piping required to reach the reservoirs that contain superheated geothermal fluids above 500K, and may offset the effects of the higher temperatures in the sample data. The trends in Figures 5 and 6 are interrelated, as η_B noticeably drops off for production wells above 3000m there is a corresponding positive increase in Figure 6a for $E_{net/well}$ as a function of D_{well}. This suggests that T_{res} values above 500K, the transition point from moderate to high enthalpy systems, are associated with well depths exceeding 3000m, and that despite the corresponding exergy losses of a deeper well, the power output caused by a higher T_{res} offsets these losses to produce the positive trend seen in Figure 5a. In simple terms, tapping a hot reservoir is more important than tapping a shallow one - though in practice this is highly limited by the economics of drilling, and thus temperature should prioritized until the point at which drilling deeper begins to offset the net power output gains.

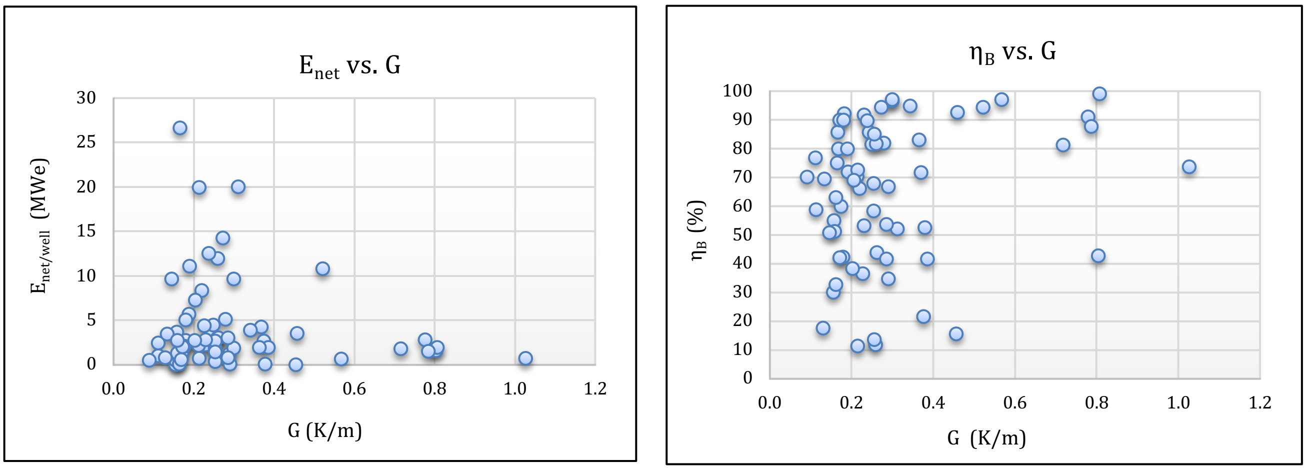

Figure 7. (a) *$E_{net/well}$ as a function of G* **(b)** *η_B as a function of G.*

Following on from the relation of T_{res} to D_{well}, the plots of G vs. $E_{net/well}$ and η_B in Figure 7 represent a normalization of the parameters seen in Figures 5 and 6 as thermal gradient was calculated as a function of T_{res} and D_{well}. Figure 7a exhibits an L shape trend, with a high clustering of data points close to the y and x axes suggesting that a majority of geothermal systems utilize production wells with low thermal gradients (approx. 0.2 K/m) and produce outputs in region of 1-5MWe per well.

In addition to signifying homogeneity in production wells, the low $E_{net/well}$ values of the >0.4K/m thermal gradients hint at one of the following conclusions. Geothermal systems are either not designed in a manner that takes advantage of thermal gradient, or thermal gradient has no correlation to $E_{net/well}$ in our data. This, as theorized, is attributed to the fact that T_{res} and D_{well} increase proportionally, and thus small gradient values are returned by the normalization calculation and no trend is exhibited. Figure 7b similarly has significant clustering of data in the same gradient region as 7a, simply indicating that most G values for geothermal systems are <0.4K/m and a full spectrum of η_B values are found in this range.

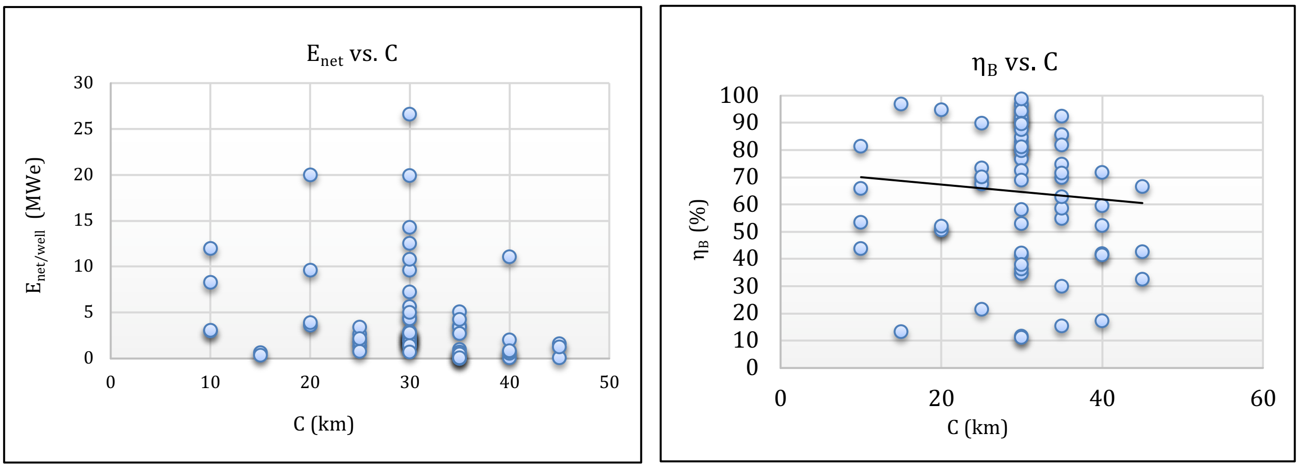

Figure 8. (a) *$E_{net/well}$ as a function of C* **(b)** *η_B as a function of C.*

Figure 8a displays $E_{net/well}$ as a function of C, appearing to exhibit a rough bell-shape curve - with noticeably low outputs for 25 and 35km thicknesses. This may be due to specialised plate tectonics in the geographical regions, further highlighted by the fact that four out of five of the 25km facilities are located in Japan. This trend requires further investigation as the majority of data values were of facilities with 30km thickness, and thus may be skewing the data away from the actual influence of C on electrical output. Examining equal numbers of facilities from each thickness category would allow for a more measured comparison between them. There was however a slight negative trend for η_B vs. C, with a noticeable drop in the upper limit exergy values that dropped from 100% at 30km to 65% at 45km.

Referring to the table in Appendix 1, most of the 40km > C values corresponded to D_{well} values exceeding 2500m. These deep reservoirs were found to correspond to higher exergy losses, and thus may account for this trend seen in 8b - further analysis is required to conclude whether crust thickness or depth is responsible for the trend line produced.

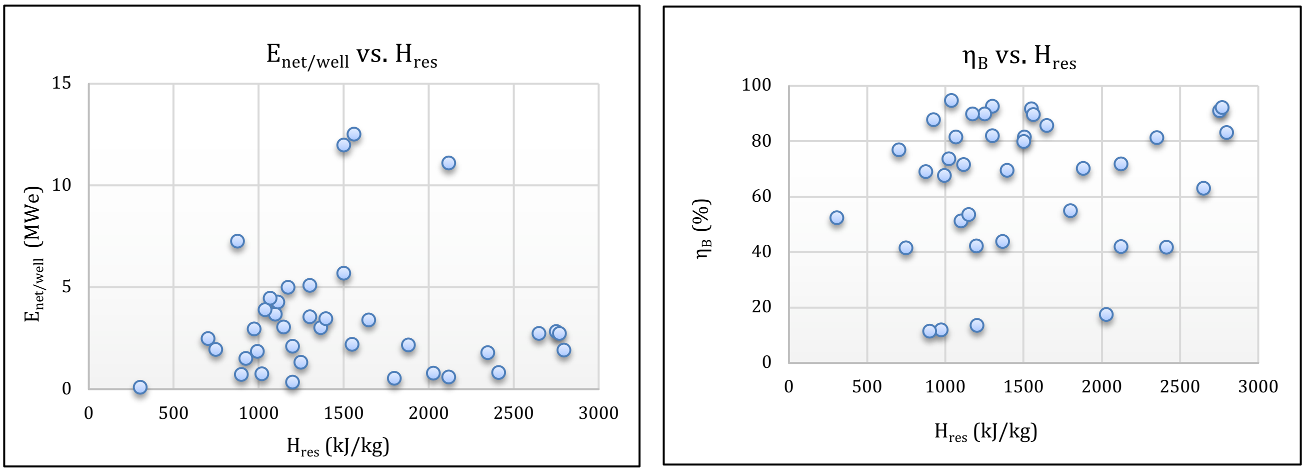

Figure 9. (a) *$E_{net/well}$ as a function of H_{res}* **(b)** *η_B as a function of H_{res}.*

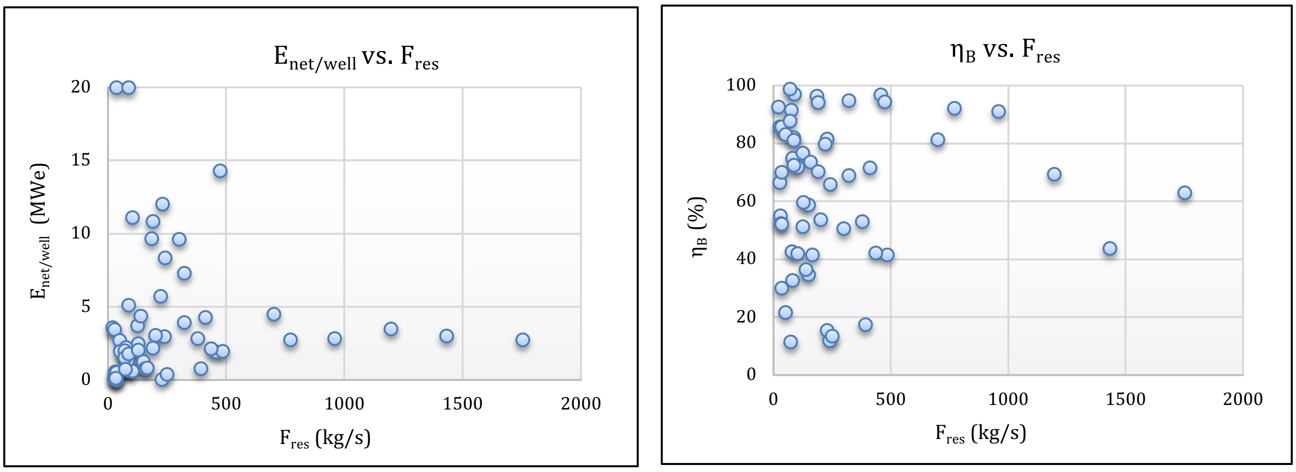

Figure 10. (a) *$E_{net/well}$ as a function of F_{res}* **(b)** *η_B as a function of F_{res}.*

Plots 9 and 10 examine the relation of H_{res} and F_{res} to $E_{net/well}$ and η_B. H_{res} has a near identical trend in both of its plots to Figure 5 as the equation for enthalpy relies heavily on the influence of temperature, and thus they cannot be viewed separately. F_{res} has a near identical trend to that of Figure 7, and similarly may be suggesting that this parameter has a tertiary influence on output metrics for a geothermal system.

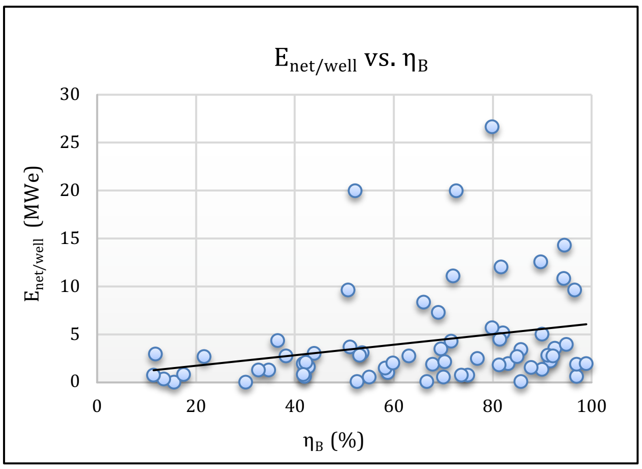

Figure 11. *$E_{net/well}$ as a function of η_B.*

Figure 11 represents the overall relation between the output and exergy efficiency of a geothermal system, exhibiting a proportional correlation. This graph essentially confirms the data utilized in the meta-study is correct for a steam turbine system, as power output is expected to increase as more energy makes it through the system. Appendix 1 contains plots of all combinations of reservoir parameters, undertaken as an attempt to determine whether normalization was possible. Thermal Gradient, taken from the plot of Appendix C, was the only normalization displayed in the results and thus the rest were excluded from the main body. The trends exhibited in these figures are all established in the literature and accounted for thoroughly by thermodynamic theory, or explained better by the plots above. The strength of the trends identified in Figure 5a (T_{res}) and Figure 6b (D_{well}) lead to the classification of these reservoir parameters as being primary in nature, in that they have the most direct influence on $E_{net/well}$ and η_B, respectively. Figures 6a (D_{well}) and 8b (C) represent the secondary parameters that have a significantly lesser, though not insignificant, relation to $E_{net/well}$ and η_B, respectively. The trends suggest that production wells in prospective geothermal fields should be considered primarily by their maximum geothermal fluid temperature, with an attempt made to choose reservoirs requiring the smallest length of piping to reduce exergy losses.

4. Conclusions

The strength of the trends identified in Figure 5a (T_{res}) and Figure 6b (D_{well}) lead to the classification of these reservoir parameters as being primary in nature, in that they have the most direct influence on $E_{net/well}$ and η_B, respectively. Figures 6a (D_{well}) and 7b (C) represent the secondary parameters that have a significantly lesser, though not insignificant, relation to $E_{net/well}$ and η_B, respectively. The clustering of output values in many plots suggests that there are well-defined barriers for output and exergy efficiency based on the current state of the technology utilized in geothermal systems across the world. These barriers represent a clear hurdle for industry and research organizations to overcome through advancement of turbine efficiency and proper identification of high-production capability thermal reservoirs. This meta-study concludes that the maximum geothermal fluid temperature of a thermal reservoir should be prioritized in prospective geothermal fields. A secondary consideration should be made to choose shallow reservoirs that require the smallest length of piping, in order to reduce exergy losses.

Acknowledgments

The author would like to acknowledge Dr. Jurgen Schulte, Dr. Martin Bell, Joshua Pritchard, Blake Regan, fellow Energy Science & Technology students and the University of Technology Sydney for guidance and assistance in the construction and peer-reviewing process of this meta-study.

References and Notes

1. Gando A, Dwyer DA, McKeown, RD, Zhang C (2011). Partial radiogenic heat model for Earth revealed by geoneutrino measurements. Nature Geoscience 4:647. doi:10.1038/ngeo1205. Gando A, Dwyer DA, McKeown, RD, Zhang C (2011). Partial radiogenic heat model for Earth revealed by geoneutrino measurements. Nature Geoscience 4:647. doi:10.1038/ngeo1205.
2. DW (GER) Geothermal energy: why hasn't it caught on yet? [Internet]. [cited 2018 May 10]. Available from: http://www.dw.com/en/geothermal-energy-why-hasnt-it-caught-on-yet/a-40487029
3. Geothermal Energy Association (USA) Geothermal basics - environmental benefits [Internet]. [cited 2018 May 8]. Available from: http://geo-energy.org/geo_basics_environment.aspx
4. Office of Energy Efficiency & Renewable Energy (USA) Geothermal power plants - minimizing solid waste and recovering minerals [Internet]. [cited 2018 May 10]. Available from: https://www.energy.gov/eere/geothermal/geothermal-power-plants-minimizing-solid-waste-and-recovering-minerals

5. Axellson G. Role and management of geothermal reinjection. 2012; Short Course on Geothermal Development and Geothermal Wells: 1-21
6. Eliasson EI (2001). Power Generation from High-Enthalpy Geothermal Resources. GHC Bulletin 1:26-34
7. Office of Energy Efficiency & Renewable Energy (USA) Energy 101: Geothermal Energy [Internet]. [cited 2018 May 10]. Available from: https://www.energy.gov/eere/videos/energy-101-geothermal-energy
8. IEA (FRA) Renewable Energy Essentials: Geothermal [Internet]. [cited May 12]. Available from: https://www.iea.org/publications/freepublications/publication/Geothermal_Essentials.pdf
9. Sanyal SK (2004). Cost of Geothermal Power and Factors That Affect It. Twenty-Ninth Workshop on Geothermal Reservoir Engineering 1-9
10. "Geothermal Basics Overview". Office of Energy Efficiency and Renewable Energy. Archived from the original on 4 October 2008. Retrieved 1 October 2008.
11. https://ac-els-cdn-com.ezproxy.lib.uts.edu.au/S0196890413007085/1-s2.0-S0196890413007085-main.pdf?_tid=f3e145c8-2fde-4c7e-97f2-6d245c9865e1&acdnat=1526889926_52d30a920aa869a4f9b1760fbd8ab8a5
12. Thermodynamic Optimization of a Geothermal- Based Organic Rankine Cycle System Using an Artificial Bee Colony Algorithm Osman Özkaraca; Keçebaş, Pınar; Demircan, Cihan; Keçebaş, Ali. Energies; Basel Vol. 10, Iss. 11, (2017): 1691.
13. https://www-inderscienceonline-com.ezproxy.lib.uts.edu.au/doi/pdf/10.1504/IJEX.2013.052543
14. https://en.wikipedia.org/wiki/File:Diagram_HotWaterGeothermal_inturperated_version.svg
15. https://en.wikipedia.org/wiki/File:Geothermal_Binary_System.svg
16. https://renewnrg.blogspot.com.au/2018/02/report-100-renewable-energy-with-grid.html
17. Tester, Jefferson W. (Massachusetts Institute of Technology); et al., The Future of Geothermal Energy (PDF), Impact, of Enhanced Geothermal Systems (Egs) on the United States in the 21st Century: An Assessment, Idaho Falls: Idaho National Laboratory, ISBN 0-615-13438-6, retrieved 7 February 2007
18. https://onlineacademiccommunity.uvic.ca/2060project/2017/06/29/why-arent-we-using-geothermal-energy-for-electricity-in-canada/
19. DiPippo, R. (2004) 'Second law assessment of binary plants generating power from lowtemperature geothermal fluids', Geothermics, Vol. 33, pp.565–586. https://doi.org/10.1016/j.geothermics.2003.10.003
20. http://www.petratherm.com.au/FAQRetrieve.aspx?ID=36536 + Lund, John W. (June 2007), Characteristics, Development and utilization of geothermal resources (PDF), Geo-Heat Centre Quarterly Bulletin, Klamath Falls, Oregon: Oregon Institute of Technology, 28 (2), pp. 1–9, ISSN 0276-1084, retrieved 2009-04-16
21. https://earthquake.usgs.gov/data/crust/crust.php
22. Watts-Henwooda N, Campbella KA, Lynneb BY, Guidoc DM, Rowlanda JV, Browned PRL. Snapshot of hot-spring sinter at Geyser Valley, Wairakei, New Zealand, following anthropogenic drawdown of the geothermal reservoir. 2017; Geothermics 68: 94-114. https://doi.org/10.1016/j.geothermics.2017.03.002
23. Thaina IA, Careyb B. Fifty years of geothermal power generation at Wairakei. 2009; Geothermics 38: 48-63. https://doi.org/10.1016/j.geothermics.2008.12.004
24. Bertani, R. World geothermal power generation in the period 2001–2005. 2005; Geothermics 34: 651 - 690. https://doi.org/10.1016/j.geothermics.2005.09.005
25. Breede K, Dzebisashvili K, Liu X, Falcone G. A systematic review of enhanced (or engineered) geothermal systems: past, present and future. 2013; Thermal Energy: 2-27.
26. Bertani, R. Geothermal power generation in the world 2005–2010 update report. 2012; Geothermics 41: 1-29. https://doi.org/10.1016/j.geothermics.2011.10.001
27. Lentz A, Almanza R. Solar–geothermal hybrid system. 2006; Applied Thermal Engineering 26: 1537-1544. https://doi.org/10.1016/j.applthermaleng.2005.12.008

28. Aneke M, Agnew B, Underwood C. Performance analysis of the Chena binary geothermal power plant. 2011; Applied Thermal Engineering 31: 1825-1832. https://doi.org/10.1016/j.applthermaleng.2011.02.028
29. Erkan K, Holdmann G, Benoit W, Blackwell D. Understanding the Chena Hot Springs, Alaska, geothermal system using temperature and pressure data from exploration boreholes. 2008; Geothermics 37: 565-585. https://doi.org/10.1016/j.geothermics.2008.09.001
30. Pambudi NA, Itoi R, Jalilinasrabady S, Jaelani K. Exergy analysis and optimization of Dieng single-flash geothermal power plant. 2014; Energy Conversion and Management 78: 405-411. https://doi.org/10.1016/j.enconman.2013.10.073
31. Ganjehsarabi H, Gungor A, Dincer I. Exergetic performance analysis of Dora II geothermal power plant in Turkey. 2012; Energy 46: 101-108. https://doi.org/10.1016/j.energy.2012.02.039
32. Luoa C, Huangc L, Gonga Y, Maa W. Thermodynamic comparison of different types of geothermal power plant systems and case studies in China. 2012; Renewable Energy 48: 155-160. https://doi.org/10.1016/j.renene.2012.04.037
33. Yahara T, Tokita H. Sustainability of the Hatchobaru geothermal field, Japan. 2010; Geothermics 39: 382-390. https://doi.org/10.1016/j.geothermics.2010.09.001
34. Noorollahi Y, Itoi R. Production capacity estimation by reservoir numerical simulation of northwest (NW) Sabalan geothermal field, Iran. 2011; Energy 36: 4552-4569. https://doi.org/10.1016/j.energy.2011.03.046
35. DiPippoa R, Moyab P. Las Pailas geothermal binary power plant, Rincón de la Vieja, Costa Rica: Performance assessment of plant and alternatives. 2013; Geothermics 48: 1-15. https://doi.org/10.1016/j.geothermics.2013.03.006
36. New Zealand : 100 MW Ngatamariki Geothermal Power Plant in New Zealand completed by Ormat. MENA Report 2013 Sep 05.
37. Prevost, JK-J. The Geothermal Energy Industry of El Salvador. 2004; Sustainable Energy Spring: 1-22.
38. Austria, JJC JR. Production capacity assessment of the Bacon-Manito geothermal reservoir, Philippines. 2008; MSc thesis Department of Mechanical and Industrial Engineering University of Iceland: 1-89.
39. Herrera, CAM. Geothermal and Solar Energy in Cerro Prieto. 2015; Proceedings World Geothermal Congress: 1-7.
40. Holdmann, G. The Chena Hot Springs 400kW Geothermal Power Plant: Experience gained during the first year of operation. 2009: 1-9.
41. Huang, L. The case studies of mid-low temperature geothermal power plant in China. 2015; Proceedings World Geothermal Congress: 1-7.
42. Bjornsson, S. Geothermal Development and Research in Iceland. 2006; National Energy Authority and Ministries of Industry and Commerce: 1-40.
43. Sigfusson B, Gunnarsson I. Scaling prevention experiments in the Hellisheidi power plant, Iceland. 2011; Thirty-Sixth Workshop on Geothermal Reservoir Engineering: 1-5.
44. Horie T, Muto T, Gray T. Technical Features of Kawerau Geothermal Power Station, New Zealand. 2010; Proceedings World Geothermal Congress: 1-4.
45. Flores-Armenta M, Gutiérrez-Negrín L. Geothermal Activity and Development in Mexico. 2011; Short Course on Geothermal Drilling, Resource Development and Power Plants: 1-12.
46. Nielsen G, Maack R, GudmundssonA, Gunnarsson GI. Completion of Krafla geothermal power plant. 2000; Proceedings World Geothermal Congress: 1-7.
47. Razzano F, Cei M. Geothermal power generation in Italy 2010-2014 update Report. 2015; Proceedings World Geothermal Congress: 1-10.
48. Emoricha EB, Omagbon JB, Malate RCM. Three dimensional numerical modeling of Mindanao geothermal production Field, Philippines. 2010; Thirty-Fifth Workshop on Geothermal Reservoir Engineering: 1-7.

49. Moya P, DiPippo R. Miravalles Unit 3 Single-Flash Plant, Guanacaste, Costa Rica: Technical and Environmental Performance Assessment. 2011; Short Course on Geothermal Drilling, Resource Development and Power Plants: 1-11.
50. Hanano M, Kajiwara T, Hishi Y, Arai F, Asanuma M, Sato K, Takanohashi M. Overview of Production at the Mori Geothermal Field, Japan. 2005; Proceedings World Geothermal Congress: 1-11.
51. Ballzus C, Frimannson H, Gunnarsson GI, Hrolfsson I. The Geothermal Power Pant at Nesjavellir, Iceland. 2000; Proceedings World Geothermal Congress: 1-6.
52. DiPippoa R, Moyab P. Las Pailas geothermal binary power plant, Rincón de la Vieja, Costa Rica: Performance assessment of plant and alternatives. 2013; Geothermics 48: 1-15. https://doi.org/10.1016/j.geothermics.2013.03.006
53. Ergon Energy (AU) Birdsville organic rankine cycle geothermal power plant [Internet]. (Cited 2018 May 15). Available from;
54. Pemecker G. Altheim geothermal plant for electricity production by ORC-turbogenerator. 2009; Bulletin d'hrydrogdologie No 17: 1-8.
55. Moya P, Nietzen F, Castro S, Taylor W. Behaviour of the geothermal reservoir at the Miravalles geothermal field during 1992-2010. 2011; Thirty-Sixth Workshop on Geothermal Reservoir Engineering: 1-20.
56. Ruiz OV. The Miravalles geothermal system, Costa Rica. 2013; Short Course V on Conceptual Modelling of Geothermal Systems: 1-29.
57. Nielsen G, Maack R, Gudmundsson A, Gunnarsson GI. Completion of Krafla geothermal power plant. 2000; Proceedings World Geothermal Congress: 1-6.
58. Reith S. Session VII: Plant operation, energy supply and grid integration Geothermal power in the reality of the electricity market. 2012; Geoelec training course Strasburg: 1-80.
59. BINE (GER) Geothermal electricity generation in Soultz-sous-Forêts [Internet]. (Cited 2018 April 13)
60. Wentao B, Bo L. Hydrochemical and Geochemical Characteristics of Geothermal Water in Gedong Area of Guizhou Province. 2017; Journal of Environmental & Analytical Toxicology: 1-6.
61. Franciso A. Reservoir assessment of Zunil I & II geothermal fields, Guatemala. 2009; Geothermal training Programme: 1-32.
62. Knapek E, Kittl G. Unterhaching power plant and overall system. 2007; Proceedings European Geothermal Congress: 1-4.
63. Seibt P, Kabus F, Bartels J, Kellner T, Hoth P. The Neustadt-Glewe Geothermal Plant: From Exploration to Successful Operation. 2010; Federal Authority for Geosciences and Natural Resources of Germany: 1-65.
64. Valdimarsson P. The Kalina power plant in Husavik - why Kalina and what has been learned. 2009; Electricity generation from Enhanced Geothermal Systems 14.-16. September in Strasbourg: 1-39.
65. Hanano M, Kajiwara T, Hishi Y, Arai F, Asanuma M, Sato K, Takanohashi M. Overview of production at the Mori geothermal field, Japan. 2005; Proceedings World Geothermal Congress: 1-10.
66. Hanano M. A quarter century of geothermal power production at Matsukawa, Japan. 2016; Japan Metals and Chemicals: 1-17.
67. Fujii Y, Saito H, Kiyota Y, Yahara T, Daibo T. Drilling make-up well (O-21) at Otake geothermal power station to maintain power output and reservoir stability. 2015; J.Geotherm. Res. Soc. Japan Vol. 37. No. 2: 1-5.
68. Garg SK, Combs J, Azawa F, Gotoh H. A study of production/injection data from slim Holes and large-diameter wells at the Takigami geothermal field, Kyushu, Japan. 1996; Contractor Report Unlimited Release: 1-302.
69. Suga, T. Recent activities of the development of geothermal energy Yuzawa City, northern part of Japan. 2017; Yuzawa city general affairs department planning section: 1-27.

70. Garcia-Gutierrez A, Martinez-Estrella JI, Ovando-Castelar R, Canchola-Félix I, Jacobo-Galvan P. Energy recovery in the Cerro Prieto geothermal field fluid transportation network. 2015; Proceedings World Geothermal Congress: 1-7
71. DW (GER) Geothermal energy: why hasn't it caught on yet? [Internet]. [cited 2018 May 10]. Available from: http://www.dw.com/en/geothermal-energy-why-hasnt-it-caught-on-yet/a-40487029
72. Geothermal Energy Association (USA) Geothermal basics - environmental benefits [Internet]. [cited 2018 May 8]. Available from: http://geo-energy.org/geo_basics_environment.aspx
73. Office of Energy Efficiency & Renewable Energy (USA) Geothermal power plants - minimizing solid waste and recovering minerals [Internet]. [cited 2018 May 10]. Available from: https://www.energy.gov/eere/geothermal/geothermal-power-plants-minimizing-solid-waste-and-recovering-minerals
74. Axellson G. Role and management of geothermal reinjection. 2012; Short Course on Geothermal Development and Geothermal Wells: 1-21
75. Eliasson EI (2001). Power Generation from High-Enthalpy Geothermal Resources. GHC Bulletin 1:26-34
76. Office of Energy Efficiency & Renewable Energy (USA) Energy 101: Geothermal Energy [Internet]. [cited 2018 May 10]. Available from: https://www.energy.gov/eere/videos/energy-101-geothermal-energy
77. IEA (FRA) Renewable Energy Essentials: Geothermal [Internet]. [cited May 12]. Available from: https://www.iea.org/publications/freepublications/publication/Geothermal_Essentials.pdf
78. Sanyal SK (2004). Cost of Geothermal Power and Factors That Affect It. Twenty-Ninth Workshop on Geothermal Reservoir Engineering 1-9
79. "Geothermal Basics Overview". Office of Energy Efficiency and Renewable Energy. Archived from the original on 4 October 2008. Retrieved 1 October 2008.
80. https://ac-els-cdn-com.ezproxy.lib.uts.edu.au/S0196890413007085/1-s2.0-S0196890413007085-main.pdf?_tid=f3e145c8-2fde-4c7e-97f2-6d245c9865e1&acdnat=1526889926_52d30a920aa869a4f9b1760fbd8ab8a5
81. Thermodynamic Optimization of a Geothermal- Based Organic Rankine Cycle System Using an Artificial Bee Colony Algorithm Osman Özkaraca; Keçebaş, Pınar; Demircan, Cihan; Keçebaş, Ali. Energies; Basel Vol. 10, Iss. 11, (2017): 1691.
82. https://www-inderscienceonline-com.ezproxy.lib.uts.edu.au/doi/pdf/10.1504/IJEX.2013.052543
83. https://en.wikipedia.org/wiki/File:Diagram_HotWaterGeothermal_inturperated_version.svg
84. https://en.wikipedia.org/wiki/File:Geothermal_Binary_System.svg
85. https://renewnrg.blogspot.com.au/2018/02/report-100-renewable-energy-with-grid.html
86. Tester, Jefferson W. (Massachusetts Institute of Technology); et al., The Future of Geothermal Energy (PDF), Impact, of Enhanced Geothermal Systems (Egs) on the United States in the 21st Century: An Assessment, Idaho Falls: Idaho National Laboratory, ISBN 0-615-13438-6, retrieved 7 February 2007
87. https://onlineacademiccommunity.uvic.ca/2060project/2017/06/29/why-arent-we-using-geothermal-energy-for-electricity-in-canada/
88. DiPippo, R. (2004) 'Second law assessment of binary plants generating power from lowtemperature geothermal fluids', Geothermics, Vol. 33, pp.565–586
89. http://www.petratherm.com.au/FAQRetrieve.aspx?ID=36536 + Lund, John W. (June 2007), Characteristics, Development and utilization of geothermal resources (PDF), Geo-Heat Centre Quarterly Bulletin, Klamath Falls, Oregon: Oregon Institute of Technology, 28 (2), pp. 1–9, ISSN 0276-1084, retrieved 2009-04-16
90. https://earthquake.usgs.gov/data/crust/crust.php
91. Watts-Henwooda N, Campbella KA, Lynneb BY, Guidoc DM, Rowlanda JV, Browned PRL. Snapshot of hot-spring sinter at Geyser Valley, Wairakei, New Zealand, following anthropogenic drawdown of the geothermal reservoir. 2017; Geothermics 68: 94-114.
92. Thaina IA, Careyb B. Fifty years of geothermal power generation at Wairakei. 2009; Geothermics 38: 48-63.

93. Bertani, R. World geothermal power generation in the period 2001–2005. 2005; Geothermics 34: 651 - 690.
94. Breede K, Dzebisashvili K, Liu X, Falcone G. A systematic review of enhanced (or engineered) geothermal systems: past, present and future. 2013; Thermal Energy: 2-27.
95. Bertani, R. Geothermal power generation in the world 2005–2010 update report. 2012; Geothermics 41: 1-29.
96. Lentz A, Almanza R. Solar–geothermal hybrid system. 2006; Applied Thermal Engineering 26: 1537-1544.
97. Aneke M, Agnew B, Underwood C. Performance analysis of the Chena binary geothermal power plant. 2011; Applied Thermal Engineering 31: 1825-1832.
98. Erkan K, Holdmann G, Benoit W, Blackwell D. Understanding the Chena Hot Springs, Alaska, geothermal system using temperature and pressure data from exploration boreholes. 2008; Geothermics 37: 565-585.
99. Pambudi NA, Itoi R, Jalilinasrabady S, Jaelani K. Exergy analysis and optimization of Dieng single-flash geothermal power plant. 2014; Energy Conversion and Management 78: 405-411.
100. Ganjehsarabi H, Gungor A, Dincer I. Exergetic performance analysis of Dora II geothermal power plant in Turkey. 2012; Energy 46: 101-108.
101. Luoa C, Huangc L, Gonga Y, Maa W. Thermodynamic comparison of different types of geothermal power plant systems and case studies in China. 2012; Renewable Energy 48: 155-160.
102. Yahara T, Tokita H. Sustainability of the Hatchobaru geothermal field, Japan. 2010; Geothermics 39: 382-390.
103. Noorollahi Y, Itoi R. Production capacity estimation by reservoir numerical simulation of northwest (NW) Sabalan geothermal field, Iran. 2011; Energy 36: 4552-4569.
104. DiPippoa R, Moyab P. Las Pailas geothermal binary power plant, Rincón de la Vieja, Costa Rica: Performance assessment of plant and alternatives. 2013; Geothermics 48: 1-15.
105. New Zealand : 100 MW Ngatamariki Geothermal Power Plant in New Zealand completed by Ormat. MENA Report 2013 Sep 05.
106. Prevost, JK-J. The Geothermal Energy Industry of El Salvador. 2004; Sustainable Energy Spring: 1-22.
107. Austria, JJC JR. Production capacity assessment of the Bacon-Manito geothermal reservoir, Philippines. 2008; MSc thesis Department of Mechanical and Industrial Engineering University of Iceland: 1-89.
108. Herrera, CAM. Geothermal and Solar Energy in Cerro Prieto. 2015; Proceedings World Geothermal Congress: 1-7.
109. Holdmann, G. The Chena Hot Springs 400kW Geothermal Power Plant: Experience gained during the first year of operation. 2009: 1-9.
110. Huang, L. The case studies of mid-low temperature geothermal power plant in China. 2015; Proceedings World Geothermal Congress: 1-7.
111. Bjornsson, S. Geothermal Development and Research in Iceland. 2006; National Energy Authority and Ministries of Industry and Commerce: 1-40.
112. Sigfusson B, Gunnarsson I. Scaling prevention experiments in the Hellisheidi power plant, Iceland. 2011; Thirty-Sixth Workshop on Geothermal Reservoir Engineering: 1-5.
113. Horie T, Muto T, Gray T. Technical Features of Kawerau Geothermal Power Station, New Zealand. 2010; Proceedings World Geothermal Congress: 1-4.
114. Flores-Armenta M, Gutiérrez-Negrín L. Geothermal Activity and Development in Mexico. 2011; Short Course on Geothermal Drilling, Resource Development and Power Plants: 1-12.
115. Nielsen G, Maack R, GudmundssonA, Gunnarsson GI. Completion of Krafla geothermal power plant. 2000; Proceedings World Geothermal Congress: 1-7.
116. Razzano F, Cei M. Geothermal power generation in Italy 2010-2014 update Report. 2015; Proceedings World Geothermal Congress: 1-10.

117. Emoricha EB, Omagbon JB, Malate RCM. Three dimensional numerical modeling of Mindanao geothermal production Field, Philippines. 2010; Thirty-Fifth Workshop on Geothermal Reservoir Engineering: 1-7.
118. Moya P, DiPippo R. Miravalles Unit 3 Single-Flash Plant, Guanacaste, Costa Rica: Technical and Environmental Performance Assessment. 2011; Short Course on Geothermal Drilling, Resource Development and Power Plants: 1-11.
119. Hanano M, Kajiwara T, Hishi Y, Arai F, Asanuma M, Sato K, Takanohashi M. Overview of Production at the Mori Geothermal Field, Japan. 2005; Proceedings World Geothermal Congress: 1-11.
120. Ballzus C, Frimannson H, Gunnarsson GI, Hrolfsson I. The Geothermal Power Pant at Nesjavellir, Iceland. 2000; Proceedings World Geothermal Congress: 1-6.
121. DiPippoa R, Moyab P. Las Pailas geothermal binary power plant, Rincón de la Vieja, Costa Rica: Performance assessment of plant and alternatives. 2013; Geothermics 48: 1-15.
122. Ergon Energy (AU) Birdsville organic rankine cycle geothermal power plant [Internet]. (Cited 2018 May 15). Available from;
123. Pemecker G. Altheim geothermal plant for electricity production by ORC-turbogenerator. 2009; Bulletin d'hrydrogdologie No 17: 1-8.
124. Moya P, Nietzen F, Castro S, Taylor W. Behaviour of the geothermal reservoir at the Miravalles geothermal field during 1992-2010. 2011; Thirty-Sixth Workshop on Geothermal Reservoir Engineering: 1-20.
125. Ruiz OV. The Miravalles geothermal system, Costa Rica. 2013; Short Course V on Conceptual Modelling of Geothermal Systems: 1-29.
126. Nielsen G, Maack R, Gudmundsson A, Gunnarsson GI. Completion of Krafla geothermal power plant. 2000; Proceedings World Geothermal Congress: 1-6.
127. Reith S. Session VII: Plant operation, energy supply and grid integration Geothermal power in the reality of the electricity market. 2012; Geoelec training course Strasburg: 1-80.
128. BINE (GER) Geothermal electricity generation in Soultz-sous-Forêts [Internet]. (Cited 2018 April 13)
129. Wentao B, Bo L. Hydrochemical and Geochemical Characteristics of Geothermal Water in Gedong Area of Guizhou Province. 2017; Journal of Environmental & Analytical Toxicology: 1-6.
130. Franciso A. Reservoir assessment of Zunil I & II geothermal fields, Guatemala. 2009; Geothermal training Programme: 1-32.
131. Knapek E, Kittl G. Unterhaching power plant and overall system. 2007; Proceedings European Geothermal Congress: 1-4.
132. Seibt P, Kabus F, Bartels J, Kellner T, Hoth P. The Neustadt-Glewe Geothermal Plant: From Exploration to Successful Operation. 2010; Federal Authority for Geosciences and Natural Resources of Germany: 1-65.
133. Valdimarsson P. The Kalina power plant in Husavik - why Kalina and what has been learned. 2009; Electricity generation from Enhanced Geothermal Systems 14.-16. September in Strasbourg: 1-39.
134. Hanano M, Kajiwara T, Hishi Y, Arai F, Asanuma M, Sato K, Takanohashi M. Overview of production at the Mori geothermal field, Japan. 2005; Proceedings World Geothermal Congress: 1-10.
135. Hanano M. A quarter century of geothermal power production at Matsukawa, Japan. 2016; Japan Metals and Chemicals: 1-17.
136. Fujii Y, Saito H, Kiyota Y, Yahara T, Daibo T. Drilling make-up well (O-21) at Otake geothermal power station to maintain power output and reservoir stability. 2015; J.Geotherm. Res. Soc. Japan Vol. 37. No. 2: 1-5.
137. Garg SK, Combs J, Azawa F, Gotoh H. A study of production/injection data from slim Holes and large-diameter wells at the Takigami geothermal field, Kyushu, Japan. 1996; Contractor Report Unlimited Release: 1-302.
138. Suga, T. Recent activities of the development of geothermal energy Yuzawa City, northern part of Japan. 2017; Yuzawa city general affairs department planning section: 1-27.

139.Garcia-Gutierrez A, Martinez-Estrella JI, Ovando-Castelar R, Canchola-Félix I, Jacobo-Galvan P. Energy recovery in the Cerro Prieto geothermal field fluid transportation network. 2015; Proceedings World Geothermal Congress: 1-7

Appendix 1 - Data Table

Geothermal System, Country	Type	Wells	Ecap (Mwe)	Ecap/well (Mwe)	Ecap (GWh)	Enet (Mwe)	Enet/well (Mwe)	Enet (GWh)	nb	D (m)	T (K)	G (K/m)	C (km)	F (kg/s)	H (kJ/kg)
Birdsville, Australia	BORC	1	0.1	0.120	1	0.08	0.080	0.7	67	1280	371	0.29	45	26	-
Altheim, Austria	BORC	1	1	1.000	9	0.75	0.750	7	75	2300	379	0.16	35	82	-
Fengshun, China	BORC	1	0.3	0.300	2.6	0.05	0.047	0.4	16	800	364	0.46	35	228	-
Sanshui, China	BK	6	0.01	0.002	0.09	0.003	0.001	0.03	30	2300	355	0.15	35	36	-
Las Pailas, Costa Rica	BORC	5	36	7.200	315	18	3.686	161	51	2673	423	0.16	20	124	1100
Miravalles I & II, Costa Rica	SF	3	115	38.333	1007	60	20.000	526	52	1700	528	0.31	20	35	-
Miravalles III, Costa Rica	SF	7	29	4.143	254	28	3.929	241	95	1500	513	0.34	20	321	1038
Miravalles V, Costa Rica	BORC	1	19	19.000	166	10	9.633	84	51	3000	438	0.15	20	300	-
Ahuachapan, El Salvador	DF	16	95	5.938	832	68	4.281	600	72	1500	553	0.37	35	410	1115
Berlin, El Salvador	BK	14	54	3.857	473	50	3.571	440	93	1250	573	0.46	35	20	1300
Soults-Sous-Forets, France	BORC	4	3	0.750	26	2	0.525	18	70	5260	473	0.09	35	35	-
Bruschal, Germany	BK	1	1	1.000	9	0.6	0.550	5	55	2542	396	0.16	35	29	1800
Neustadt-Glewe, Germany	BORC	2	0.2	0.105	2	0.2	0.090	1.6	86	2250	372	0.17	35	35	-
Unterhaching, Germany	BK	2	3	1.700	30	2	1.000	18	59	3500	393	0.11	35	150	-
Amatitlan, Guatemala	BORC	4	25	6.300	221	21	5.125	180	82	2000	558	0.28	35	86	1300
Zunil, Guatemala	BK	7	28	4.000	245	24	3.429	210	86	2370	573	0.24	35	26	1647
Hellisheidi, Iceland	DF	44	303	6.886	2654	133	3.023	1165	44	2195	573	0.26	10	1431	1365
Husavik, Iceland	BK	3	2	0.667	18	2	0.647	17	97	700	397	0.57	15	90	-
Krafla, Iceland	SF	22	60	2.727	526	8	0.368	71	14	2200	560	0.25	15	249	1200
Nesjavellir, Iceland	SF	10	147	14.700	1288	120	12.000	1051	82	2200	573	0.26	10	229	1503
Reykjanes, Iceland	SF	12	150	12.500	1314	100	8.333	876	66	2700	593	0.22	10	241	-
Svartsengi, Iceland	SF	13	74	5.723	652	40	3.069	350	54	1800	513	0.29	10	200	1148
Dieng, Indonesia	SF	5	60	12.000	526	22	4.380	192	37	2000	453	0.23	30	139	-
Meshkinshahr, Iran	SF	9	36	4.000	315	12	1.308	103	33	3197	513	0.16	45	82	-
Larderello, Italy	DF	200	595	2.973	5208	548	2.740	4800	92	3000	543	0.18	30	771	2770
Hatchobaru, Japan	DF	20	110	5.500	964	90	4.480	785	81	2300	573	0.25	30	700	1068
Kakkonda, Japan	SF	29	80	2.759	701	54	1.870	475	68	2500	633	0.25	25	-	992
Matsukawa, Japan	SF	10	24	2.350	206	20	1.950	171	83	1300	473	0.36	30	51	2797
Mori, Japan	SF	10	50	5.000	438	21	2.112	185	42	3000	533	0.18	30	434	1199
Nigorikawa, Japan	BK	4	50	12.500	438	11	2.700	95	22	1100	413	0.38	25	50	-
Ogiri, Japan	SF	15	30	2.000	263	30	1.979	260	99	500	403	0.81	30	69	-
Onikobe, Japan	SF	12	13	1.042	110	9	0.767	81	74	500	513	1.03	25	158	1020
Otake, Japan	SF	4	13	3.125	110	11	2.655	93	85	1976	503	0.25	30	-	-
Sumikawa, Japan	SF	7	50	7.143	438	40	5.707	350	80	2500	473	0.19	30	221	1500
Takigami, Japan	SF	16	28	1.750	245	25	1.531	215	88	600	471	0.79	30	69	925
Uenotai, Japan	SF	13	29	2.215	252	23	1.800	205	81	800	573	0.72	30	86	2350
Yamagawa, Japan	SF	12	30	2.500	263	17	1.456	153	58	2100	533	0.25	30	-	-
Yanaizu-Nishiyama, Japan	SF	21	65	3.095	569	46	2.174	400	70	2600	553	0.21	25	189	1882
Olkaria I, Kenya	SF	31	185	5.968	1621	19	0.610	681	42	2500	425	0.17	40	103	2120
Olkaria II, Kenya	SF	31	105	3.387	920	63	2.025	550	60	2500	433	0.17	40	127	-
Olkaria III, Kenya	SF	9	139	15.444	1218	100	11.111	876	72	2750	523	0.19	40	103	2120
Cerro Prieto, Mexico	DF	164	820	5.000	7183	570	3.476	4993	70	4400	588	0.13	25	1195	1396
Los Azufres, Mexico	SF	43	195	4.535	1708	34	0.794	299	18	3500	453	0.13	40	391	2030
Los Humeros, Mexico	SF	20	40	2.000	350	17	0.833	146	42	2185	623	0.29	40	166	2413
Kawerau, New Zealand	DF	7	106	15.143	929	100	14.286	877	94	2100	573	0.27	30	473	-
Mokai, New Zealand	BORC	11	110	10.000	964	106	9.636	930	97	2000	599	0.30	30	184	-
Ngatamariki, New Zealand	BORC	3	100	33.333	876	80	26.637	700	80	3373	563	0.17	30	-	-
Ngawha, New Zealand	BORC	3	75	25.000	657	9	2.967	78	12	2300	593	0.26	30	239	975
Ohaaki, New Zealand	SF	23	122	5.322	1072	65	2.826	400	53	2500	573	0.23	30	378	-
Poihipi, New Zealand	SF	2	55	27.500	482	40	19.975	350	73	2300	493	0.21	30	86	-
Rotokawa, New Zealand	BORC	14	34	2.429	298	31	2.226	273	92	2500	573	0.23	30	76	1550
Te Huka, New Zealand	BORC	2	23	11.500	201	22	10.845	190	94	1100	573	0.52	30	189	-
Wairakei, New Zealand	BORC	55	171	3.109	1498	156	2.835	1365	91	660	513	0.78	30	958	2750
Momotombo, Nicaragua	DF	20	30	1.500	263	27	1.350	24	90	3000	513	0.17	25	-	1250
Bacon-Manito, Phillippines	SF	23	150	6.522	1314	17	0.743	149	11	2546	545	0.21	30	73	900
Mindanoa, Phillippines	SF	19	106	5.579	929	95	5.021	836	90	2954	533	0.18	30	-	1175
Tiwi, Phillippines	SF	48	330	6.875	2891	134	2.783	1171	38	2784	563	0.20	30	-	-
Dora I, Turkey	BORC	2	7	3.650	64	3	1.267	22	35	1517	438	0.29	30	148	-
Dora II, Turkey	BORC	5	10	1.960	86	10	1.900	83	97	1500	449	0.30	30	458	-
Kizildere, Turkey	SF	9	95	10.556	832	66	7.293	575	69	2261	463	0.20	30	321	875
Tuzla, Turkey	BORC	2	8	3.750	66	3	1.601	28	43	553	444	0.80	45	78	-
Brady Hot Springs, USA	BORC	7	33	4.700	288	14	1.957	120	42	988	381	0.39	30	484	750
Chena Hot Springs, USA	BORC	2	0.4	0.200	3.5	0.2	0.105	2	53	915	346	0.38	40	33	306
Geysers, USA	SF	350	1529	4.369	13394	963	2.752	8438	63	3200	513	0.16	35	1751	2650
Heber, USA	BORC	16	52	3.250	456	40	2.497	350	77	3928	438	0.11	30	126	702

Appendix 2 - Carnot Cycle Temperature vs. Enthalpy Plot & Integral

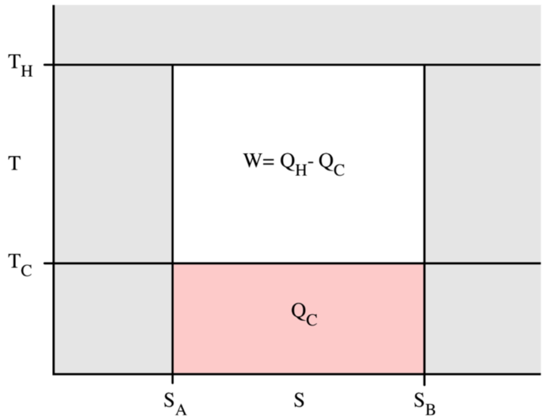

(a) *Carnot cycle process diagram, temperature (T) vs. entropy (S)* https://en.wikipedia.org/wiki/File:Carnot_Cycle2.png

$$W = \oint PdV = \oint TdS = (T_H - T_C)(S_B - S_A)$$

(b) *Carnot cycle integral describing the process shown in* **(a)**

Appendix 3 – Geothermal Parameter Dependencies

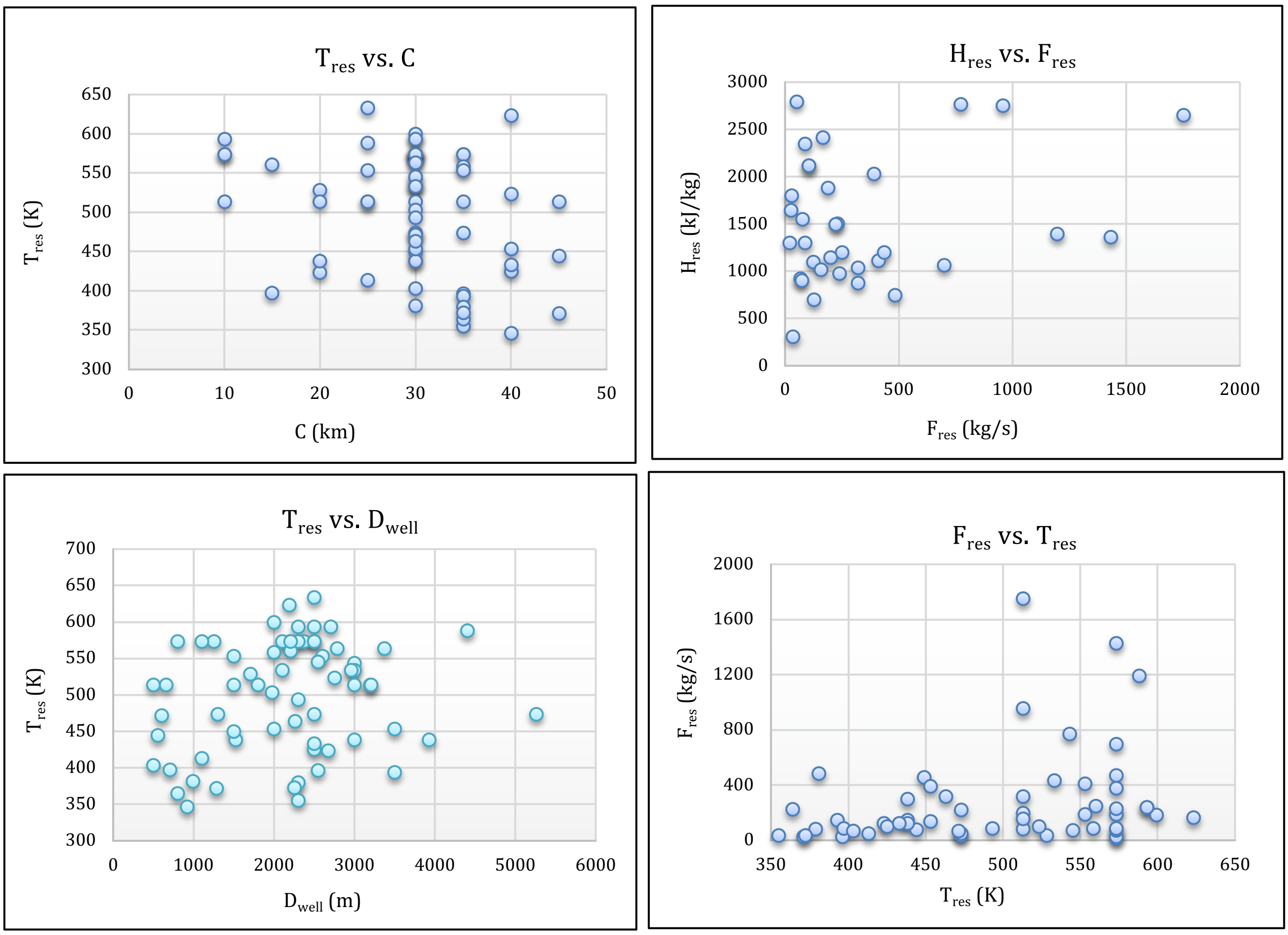

(a) T_{res} *vs. C* **(b)** H_{res} *vs.* F_{res} **(c)** T_{res} *vs.* D_{well} **(d)** F_{res} *vs.*

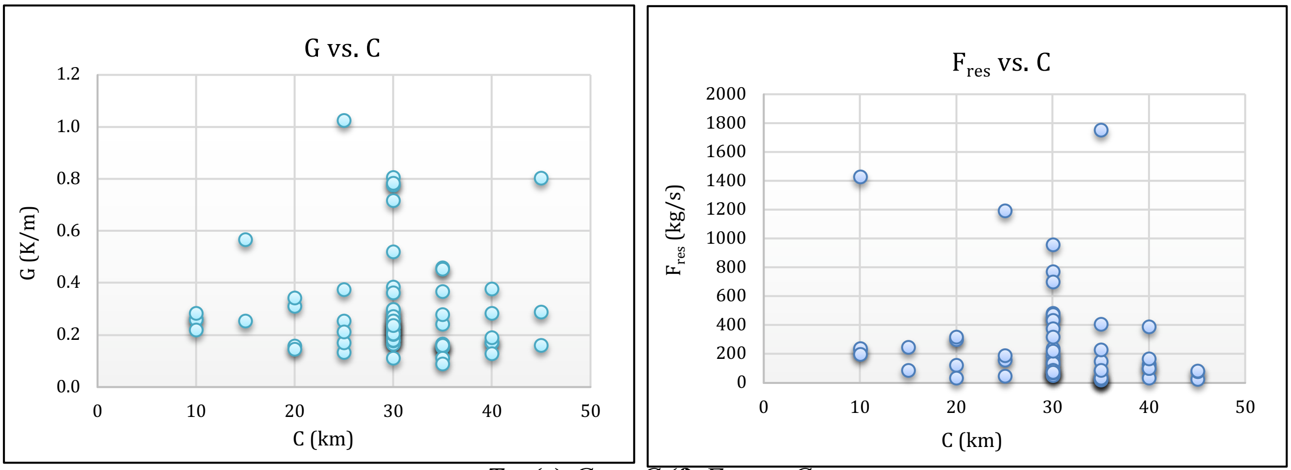

T_{res} **(e)** *G vs. C* **(f)** F_{res} *vs. C.*

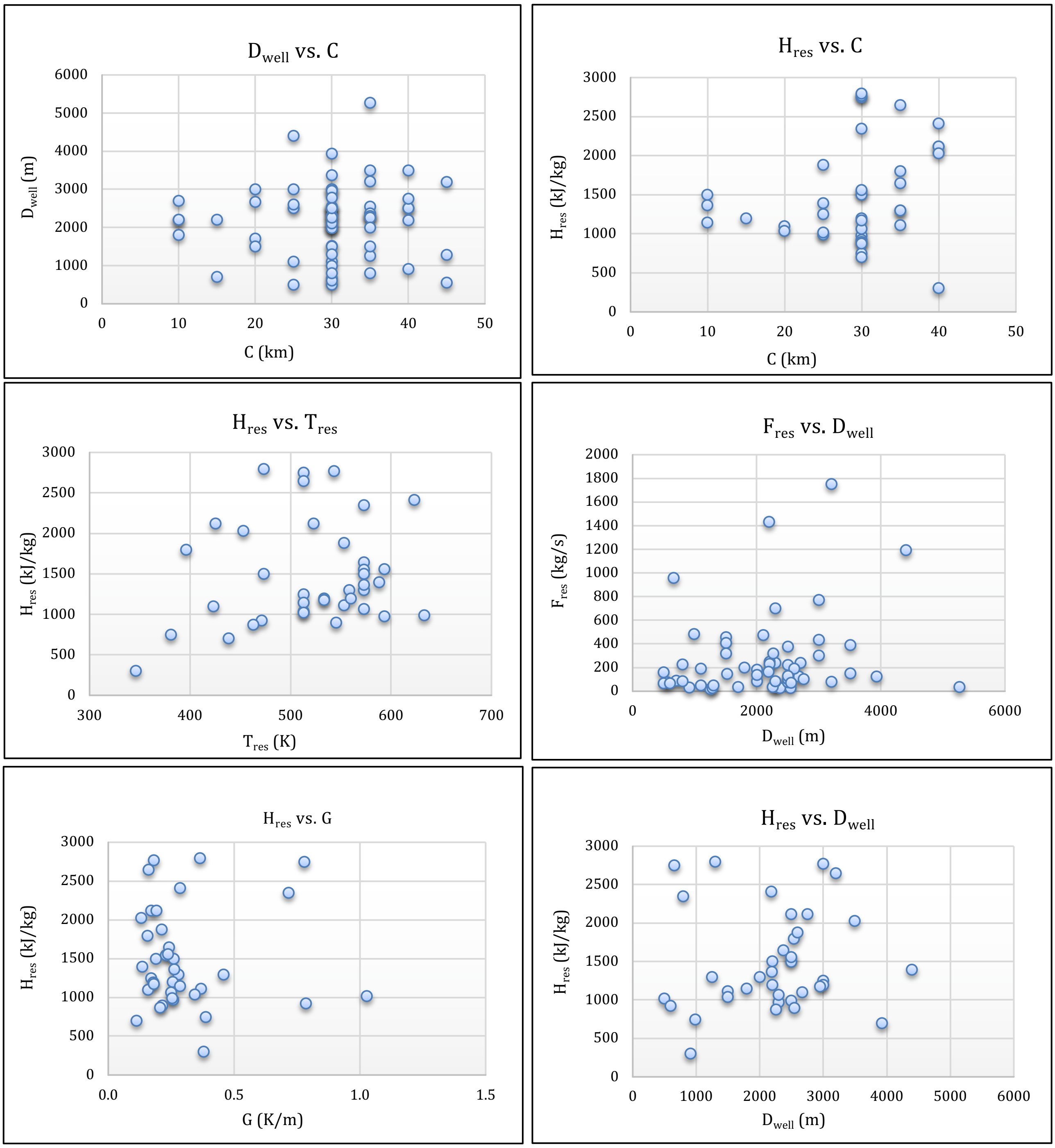

(g) D_{well} *vs. C* **(h)** H_{res} *vs. C* **(i)** H_{res} *vs.* T_{res} **(j)** F_{res} *vs.* D_{well} **(k)** H_{res} *vs. G* **(l)** H_{res} *vs.* D_{well}.

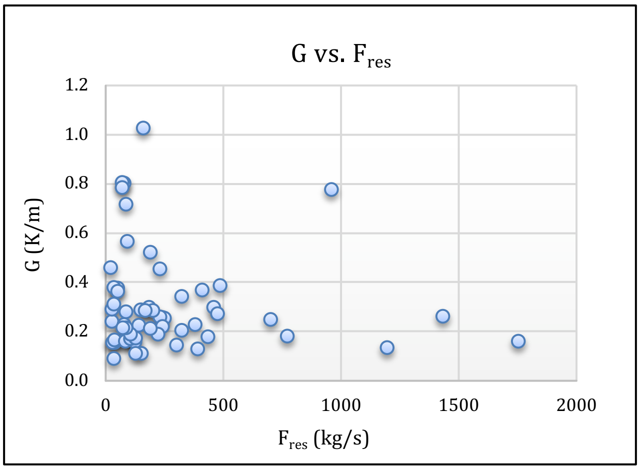

(m) G *vs.* F_{res}